scientific reports

Check for updates

OPEN

Study on polarization-insensitive splitter by combining symmetrical structure with matching layer

Wang wenliang

As the polarization state of laser can reflect more information, various types of laser remote sensing techniques have been developed. In order to accurately interpret the detection information, the optical components with polarization insensitivity has become an important topic. In this paper, a polarization insensitive splitter with three all-dielectric materials is designed and fabricated, which combines the symmetric structure with the matching layers. Statistical results show that this design has excellent performance of low polarization deviation at short wave region 420–580 nm with high reflectance and long wave region 620–880 nm with high transmittance.

Keywords Polarization insensitive, All dielectric, Symmetric structure

Optical laser technology is a very effective means of information detection, and has been playing an increasingly important role in many fields such as medicine[1], remote sensing[2] and military[3] and so on.

However, because the detection target is often in a complex environmental background, as well as the scattering and absorption of light by the medium, the detection target information will have low contrast and details will be covered, which will greatly increase the difficulty of information detection. The polarization state of light can express more information, and the technology based on the polarization state detection of light can better solve the above problems[4–6]. Full polarization remote sensing technology uses an optical system formed by a series of optical elements to obtain detailed information by identifying the changes in the polarization state of light caused by the monitoring object[7–9]. However, when oblique incidence occurs, each component of the optical system will introduce polarization deviation, which makes it difficult to interpret the information[10–12]. In order to accurately reflect the relevant information of the monitored object, the influence of the optical system on the polarization state of light should be controlled as much as possible, and the development of polarization insensitive optical regulatory devices becomes the key.

Optical coating are becoming more and more important in laser systems because they can effectively control optical properties such as intensity, phase and polarization and so on[13–15]. However, the design and manufacture of low polarization sensitivity splitters based on multilayer structures is still a challenging task due to the inherent property of polarization separation in oblique cases. Metal films have a smaller depolarizing effect than dielectrics, but the obvious absorption problem limits its use in many laser systems[16]. For the design based on all-dielectric film, the design parameters can only be provided by increasing the type of film material and the number of film layers. However, with the increase of the range of operating wavelength requirements, the difficulty of this design also increases sharply. Because the more thin film layers, the more complicated the interference problem, it is difficult to obtain an analytical design close to the design goal. As a result, the complete numerical design based on optimization algorithm often falls into local optimal due to the lack of reasonable initial value, and it is also difficult to get successful design. Even with optical film design methods such as needles that can automatically insert the film, only a large number of extremely thin film layers can be produced, which is difficult to accurately produce. Therefore, traditional designs based on metal films have very limited applications due to strong absorption. Traditional designs based on all-dielectric films typically work over a very limited wavelength range and are difficult to make successfully, and the polarization sensitivity is usually relatively high[17].

In this paper, we design a polarization-insensitive edge splitter using three kinds of all-dielectric materials and carried out experimental research. In Section "Principles and polarization control requirements", we briefly analyze the principle of polarization deviation, and illustrate the requirements of polarization control according to our practical case. The detailed design process is described in Section "Processes of design". In Section "Analysis of the design", we analyze the design results and do some experimental studies. Finally, the results are discussed in Section "Experimental research".

Xuzhou College of Industrial Technology, Xuzhou 221140, China. email: w.l.wang@163.com

Principles and polarization control requirements

As mentioned above, the stability of beam polarization state in the optical system of detection technology is an important factor affecting the accuracy of detection technology. Optical thin film devices are essential beam control elements in optical system of detection technology. However, when the light is inclined to incident on the film material, the two components of the light wave with different polarization directions will show different effective refractive indices, resulting in inevitable polarization deviation.

$$\Delta n = \frac{n_p}{n_s} = \frac{n/\cos\theta}{n\cos\theta} = \frac{1}{1-\frac{n_0^2\sin^2\theta_0}{n^2}} \tag{1}$$

Where, n_p and n_s are the effective refractive indices of the polarization components of S and P, n_0 and n are the refractive indices of the incident medium and the thin film material, θ_0 and θ are the beam inclination angles in the incident medium and thin film material, respectively. It is easy to find that the greater the tilt angle, the more severe the polarization deviation.

In our case, the role of the splitter is mainly to realize the separation of the incident beam into the transmitted light and the reflected light parts according to different frequencies. In order to equalize the polarization effect of the reflected beam and the transmitted beam, the operating angle is 45 degrees, and the different polarization components of this two beams will all show a very significant polarization deviation. This will cause a significant change in the polarization state of the beam, which will affect the accuracy of the detection system, and polarization-insensitive splitters become a critical requirement.

The broadband polarization-insensitive filter at 45° incidence presented here should have high reflectance ($\geq 95\%$) from 420 to 580 nm with Pol_{refl} less than 3.0% and high transmittance ($\geq 95\%$) from 620 to 880 nm with average Pol_{tran} less than 2.5%. Where Pol_{refl} and Pol_{tran} are the polarizations for reflectance and transmittance, which can be expressed respectively as

$$\begin{aligned} \mathrm{Pol_{reft}} &= \left|\frac{\mathrm{R_s}-\mathrm{R_p}}{\mathrm{R_s}+\mathrm{R_p}}\right| \times 100\% \\ \mathrm{Pol_{tran}} &= \left|\frac{\mathrm{T_s}-\mathrm{T_p}}{\mathrm{T_s}+\mathrm{T_p}}\right| \times 100\% \end{aligned} \tag{2}$$

The suffixes *p* and *s* used in Eq. (2) denote *p* and *s* polarization component, respectively.

Processes of design

According target about polarization control requirements as described in Part 2, the required reflection and transmission band of the filter are all comparatively wide, which cannot be obtained by a single thin film stack with two materials. However, according to the polarization control theory of optical thin films, a combination of thin film materials with relatively small polarization separation can be constructed using a variety of materials[18].

Based on characteristic matrix method[19], considering a symmetrical thin film structure with three material LMHML, which can be replaced mathematically by a virtual single-material structure with the same equivalent admittance E_{LMHML} as

$$\begin{aligned} E_{LMHML} = \Bigg\{ \Bigg[& \left(\frac{2}{n_L}+\frac{2}{n_M}+\frac{1}{n_H}\right) cos^4\delta \\ & - \left(\frac{2n_M}{n_L^2}+\frac{2n_H}{n_Ln_M}+\frac{2n_M}{n_Ln_H}+\frac{2}{n_L}+\frac{n_H}{n_L^2}+\frac{n_H}{n_M^2}\right) sin^2\delta\, cos^2\delta \\ & + \frac{n_M^2}{n_Hn_L^2} sin^4\delta \Bigg] / \Big[(2n_M+2n_L++2n_H)\, cos^4\delta \\ & - \left(\frac{2n_L^2}{n_M}+\frac{2n_Ln_M}{n_H}+\frac{2n_Ln_H}{n_M}+2n_L+\frac{n_L^2}{n_H}+\frac{n_M^2}{n_H}\right) sin^2\delta\, cos^2\delta \\ & + \frac{n_Hn_L^2}{n_M^2} sin^4\delta \Bigg] \Bigg\}^{\frac{1}{2}} \end{aligned} \tag{3}$$

When $\lambda = \lambda_0/2$, $\delta = 2\pi/\lambda_0 \cdot \lambda_0/2 = \pi$, we can get

$$E_{LMHML} = \left\{ (2n_M + 2n_L + n_H) / \left(\frac{2}{n_L}+\frac{2}{n_M}+\frac{1}{n_H}\right) \right\}^{\frac{1}{2}} \tag{4}$$

Then, in order to meet the requirements of polarization insensitivity, the refractive index of the film material must meet the matching condition

$$\Delta E_{LMHML} = \left\{ (2\Delta n_M + 2\Delta n_L + \Delta n_H) / \left(\frac{2}{\Delta n_L}+\frac{2}{\Delta n_M}+\frac{1}{\Delta n_H}\right) \right\}^{\frac{1}{2}} = 1 \tag{5}$$

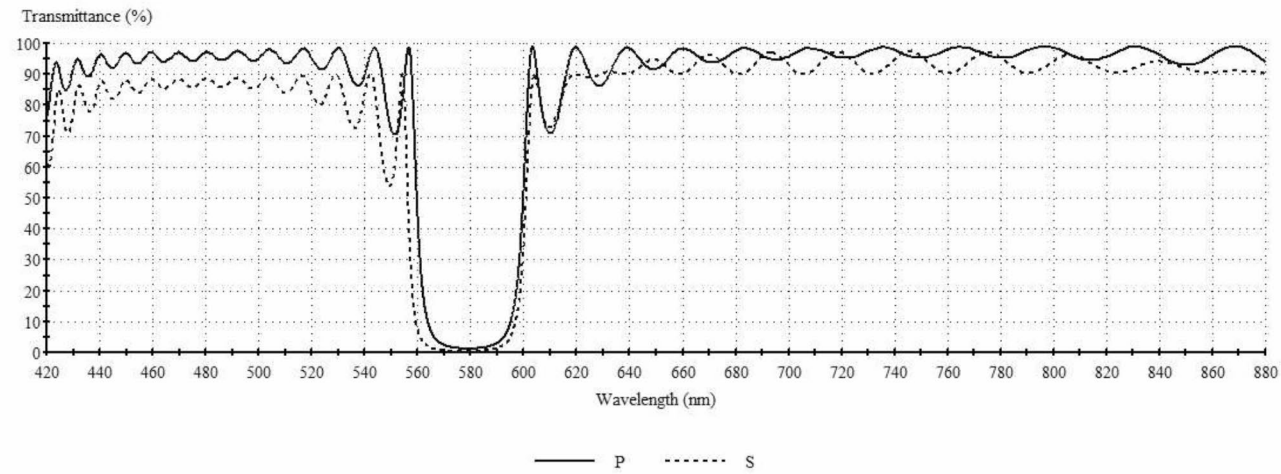

Fig. 1. Calculated spectral transmittance of the original basic stack.

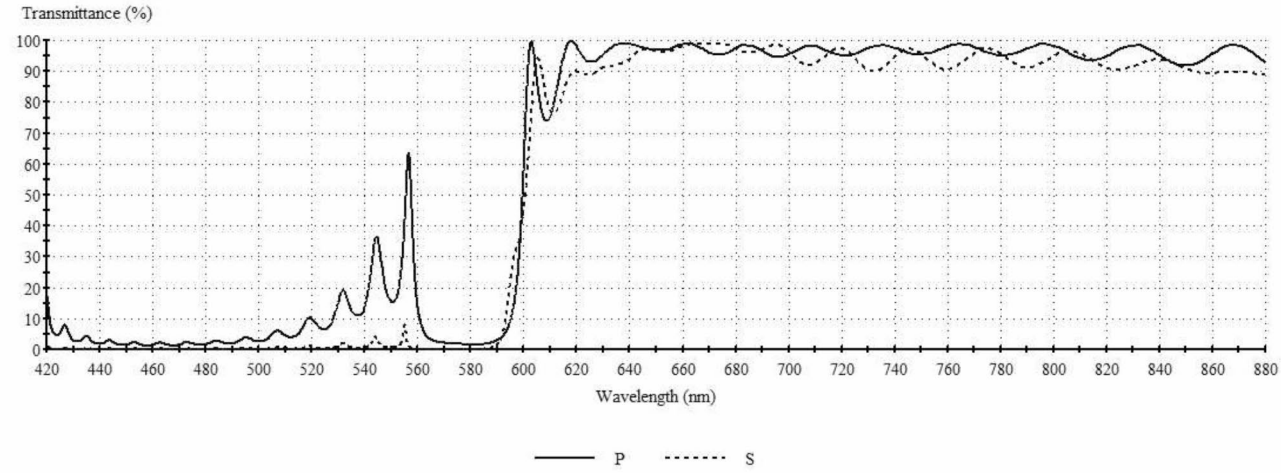

Fig. 2. Calculated spectral transmittance of the original improved stack with matching layer.

After analysis and comparison, we choose titanium dioxide, aluminum oxide and magnesium fluoride with different refractive index of high(n_H=2.34), medium(n_M=1.67) and low(n_L=1.38) respectively for polarization control. Then, when the angle of incidence is 45 degrees, according to Eq. 1,we can get Δn_H=1.10, Δn_M=1.22 and Δn_L=1.35. Under this material combination, ΔE_{LMHML}=1.06 is obtained according to Eq. 5, which is very close to 1, indicating that it is a good polarization insensitive material combination.

Then, according to the requirements of high reflectivity in the short wave region and high transmittance in the long wave region, and the working band range is relatively wide, we choose |(LMHML)^16 as the initial basic stack structure. Where H, M, and L respectively represent the quarter-wavelength optical thickness of the above three high, middle and low refractive index materials relative to the reference wavelength of 520 nm. The structure is attached to a k9 plate glass (n_S=1.52) and the incident medium is air (n_0 = 1.00) at an angle of 45 degrees. The corresponding transmittance spectral curve is shown in Fig. 1.

The calculated transmission spectral curve of the film stack has a small polarization deviation in a specific wavelength region, which can be found in Fig. 1. Especially in the long wave region, the transmittance spectral characteristics are very close to our case requirements in Section "Principles and polarization control requirements", while the polarization deviation is relatively small. However, in the shortwave region, polarization deviation becomes significantly more severe, and the transmittance spectral characteristics are far from the requirements of our case. In order to obtain better spectral transmission characteristics, a matching stacks (0.5HL0.5 H)^8 is added between the basic stack and substrate media. The corresponding transmission spectral curve of the improved structure is shown in Fig. 2.

We can obviously see that the matching layer has a very obvious role: the transmission spectral curve in the short-wave region has a great change, the overall spectral characteristics have been close to the target required by our case, except for a small part of the band still has a high transmission peak. At the same time, we are also

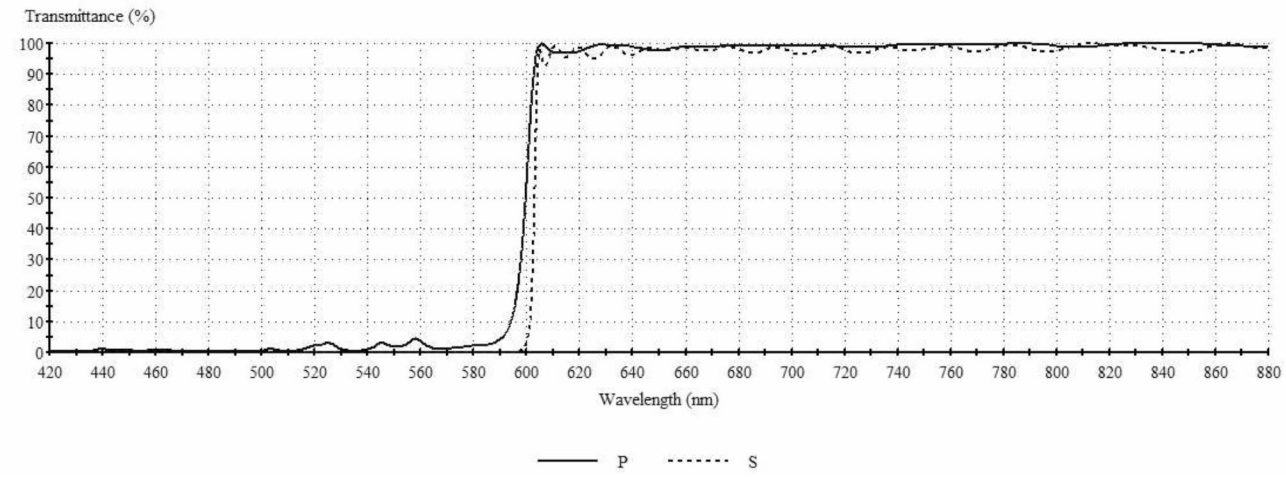

Fig. 3. Calculated spectral transmittance of the improved stack after optimization.

	420–580 nm			620–880 nm		
	Reflectance(%)			Transmittance(%)		
	P	S	Pol_{Refl}(%)	P	S	Pol_{Tran}(%)
MAX.	99.2065	99.9900	2.7797	99.9946	99.9954	2.2800
MIN.	91.9284	92.8692	0.0083	97.5250	94.8878	0.0010
AVE.	96.8038	97.8825	0.7759	99.2975	98.2491	0.5919

Table 1. Theoretical performance statistics of polarization insensitive splitter.

pleased to find that the structural improvement of the matching layer does not cause significant changes in the transmission characteristics of the long-wave region.

Then, Conjugate gradient method is used to optimize the improved stack so that the phase thickness and the optical admittances of film layers at 45° incidence could be compensated by the stack itself. After optimization, the improved structure is significantly simplified, from 82 layers to 58 layers, with a total thickness of 7. 71 microns. The corresponding transmission spectral curve of the improved structure after optimization is shown in Fig. 3 .

It should be noted that the refractive index of the material marked in all the above processes is relative to the reference wavelength of 520 nm, but due to the wide range of working bands, the design process must also consider the obvious dispersion of all materials. We measured the actual dispersion of each material according to the subsequent plasma-assisted deposition technology.

Analysis of the design

Some statistics date of the polarization insensitive splitter presented before is listed in Table 1. The average reflectance of S-polarized and P-polarized light in the short-wave region of 420 to 580 nm is 97.8825% and 96.8038% respectively. The maximum and average values of the reflectance polarization is 2.7797% and 0.7759% respectively. The average transmittance of S-polarized and P-polarized light in the long-wave region of 620 to 880 nm is 98.2491% and 99.2975% respectively. The maximum and average values of the transmittance polarization is 2.2800% and 0.5919% respectively. It can to say, in the working range of spectrum, the design maintains a very low polarization ratio.

To test the angle sensitivity for the above design, we give the calculated reflectance or transmittance curve for *P*- and *S*- polarized light when the incident angle is 42° and 48° respectively. We show this in Figs. 4 and 5. One thing must to be said before is we didn't considered the angle change in our designs process. By comparing them, we can easily find that the polarization deviation effects alter little, but the spectral band has some movement. It shows the design have a reasonable angular field.

To test the effect of filter on information, reflection group delay(GD) at short wave region 420–580 nm and transmission group delay at long wave region 620–880 nm are shown in Figs. 6 and 7 respectively. It can be found that the group delay of both working regions is very small and hardly varies with wavelength, even near the edge of the working region, the maximum group delay is below 0.12PS. These indicate that the distortion of information through the filter is very small. At the same time, we can also find that the group delay difference of different polarization components is very small, indicating that their phase delay difference is very small, which will make the filter's influence on the polarization state change of light is very small.

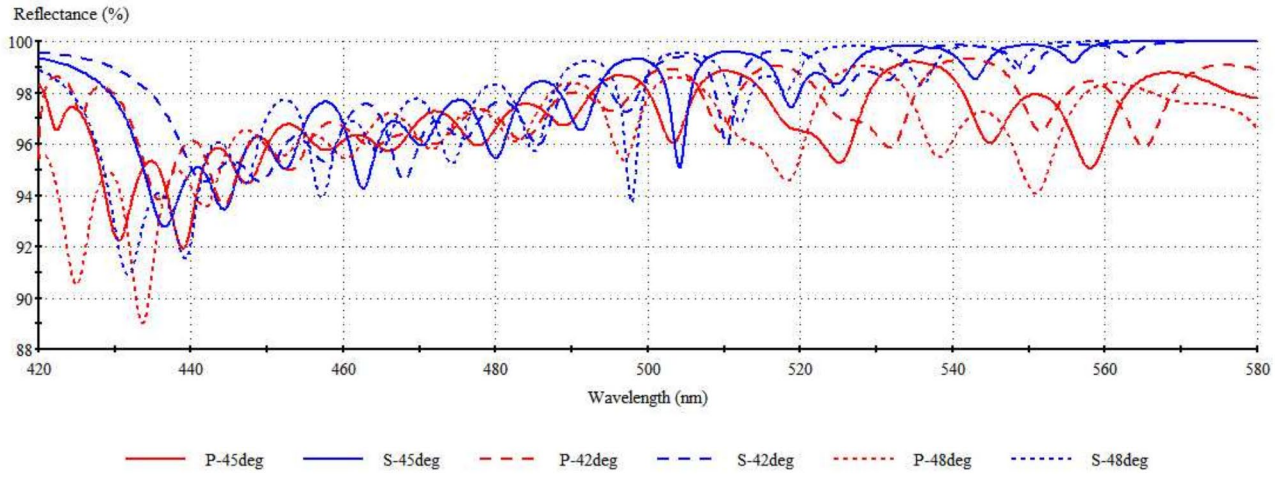

Fig. 4. Calculated reflectance curve at short wave region with incident angle is 42° and 48°.

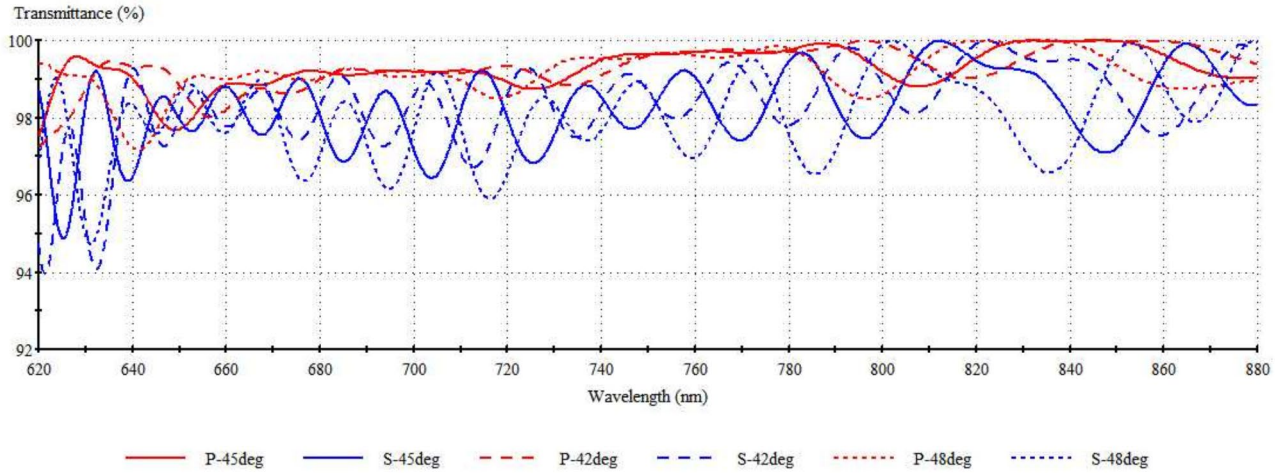

Fig. 5. Calculated transmittance curve at long wave region with incident angle is 42° and 48°.

Experimental research

Plasma-assisted evaporation deposition technology is made to deposit the above system. SYRUSpro1110 high vacuum coating machine of Leybold company used in this experiment is shown in Fig. 8, which has the capability of resistance evaporation, electron beam evaporation, and plasma assisted plating (PIAD).

Before the deposition of the layers, the glass substrate is carefully cleaned with a 1:1 mixture of ethanol and ether. When the substrate is placed in the vacuum chamber, the vacuum is pumped to 10^{-5} mbar, and the temperature is heated to 150° for baking. Then, the APS plasma source is started and the substrate is cleaned by ion beam bombardment. After the substrate treatment, the thin film material layer is deposited layer by layer, while the argon or oxygen partial pressure is maintained at 2.1×10^{-5} mbar in the vacuum chamber before deposition. All the layer thicknesses are controlled by quartz crystal oscillator monitor method.

The starting materials for the deposition of the TiO_2 layers is Ti_3O_5. The partial pressure of oxygen during deposited the TiO_2 layers is 3.8×10^{-4} mbar, and the electron-beam gun voltage and current is 6 kV and 336 mA respectively. Advanced plasma source is operated with an anode voltage of 100v and an anode current 50 mA. The rate of deposition is 0.31 nm/s.

When Al_2O_3 layer is deposited, the electron-beam gun voltage and current is 6 kV and 15 mA respectively, and there is a 2.7×10^{-4} mbar partial pressure of oxygen in the chamber during the deposition process. Advanced plasma source is operated with an anode voltage of 130v and an anode current 50 mA. The rate of deposition was 0.3 nm/s.

When MgF_2 layer is deposited, the material is laid in a molybdenum crucible, and there is a 3.05×10^{-4} mbar partial pressure of argon in the chamber during the deposition process. Advanced plasma source is operated with an anode voltage of 60v and an anode current 30 mA. The rate of deposition is 0.35 nm/s.

The final physical photo and corresponding experimental curves of the polarization insensitive splitter with working angle 45° are shown in Fig. 9a,b respectively. Compared with the theoretical calculation results, the

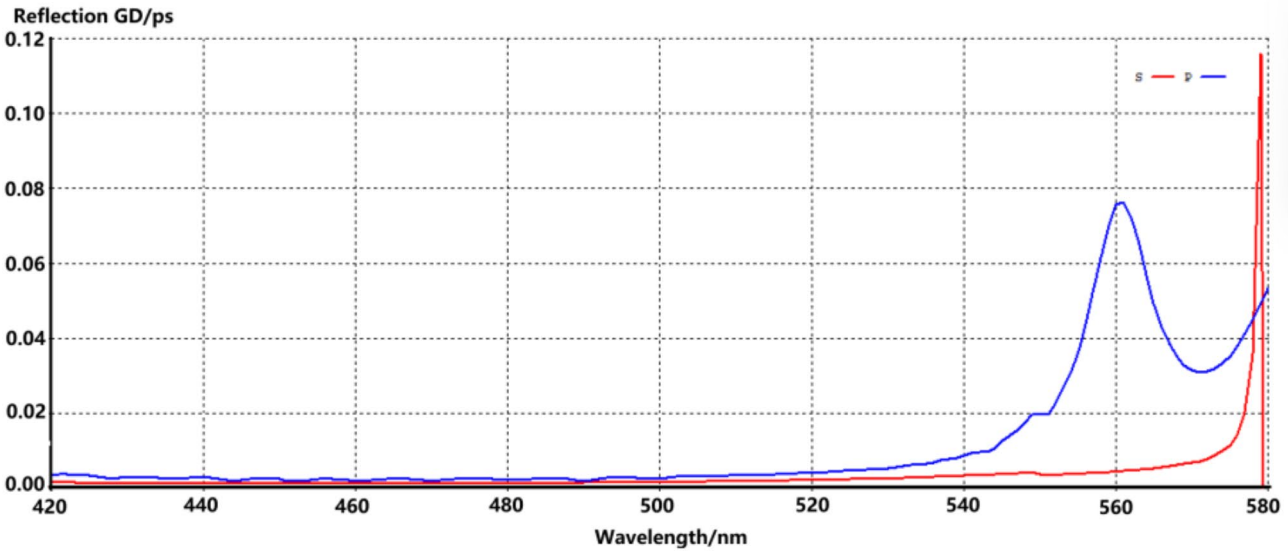

Fig. 6. Reflection GD(Group delay) at short wave region.

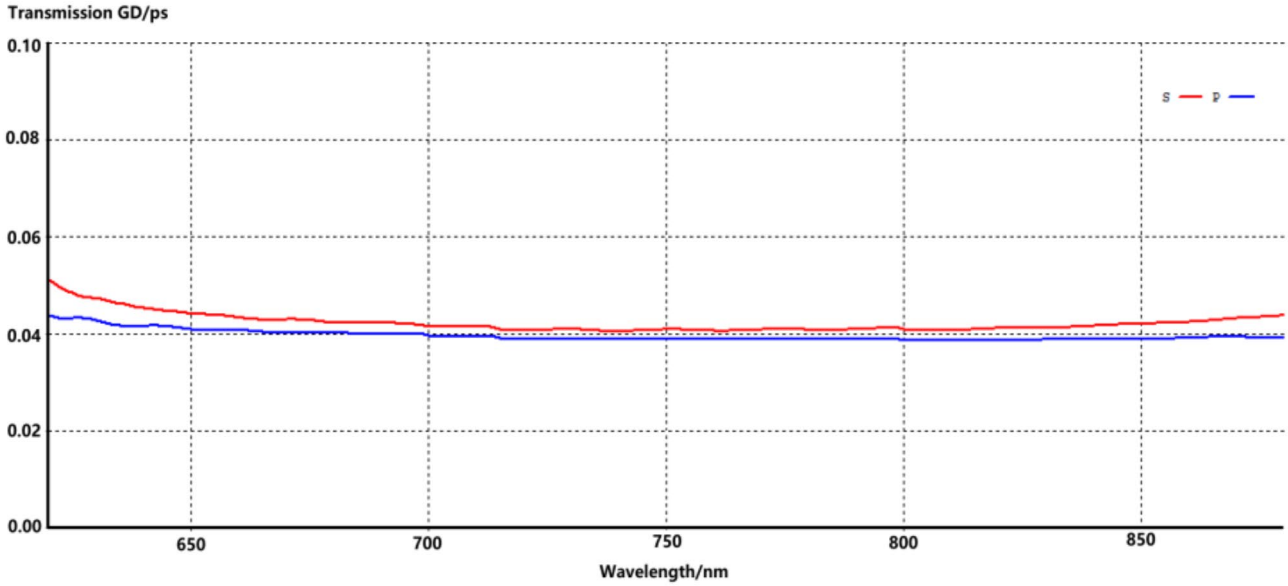

Fig. 7. Transmission GD(Group delay) at long wave region.

transmittance of the short wave region increases by about 0.8% and the reflectance decreases slightly, while the transmittance of the long wave region also decreases by about 1% at the same time. But overall, we can find that the measured curves agree very well with the calculated curves from Fig. 3. Which means that the optical performance of the polarization splitter can satisfy its requirements completely. For the influence of incident angle, we tested the transmission curve of plus or minus 3 degrees angle respectively, as shown in Fig. 9c,d respectively. When the incidence angle changes, the test transmittance curve has obvious drift. Especially when the incidence angle increases, the deterioration of the performance is more obvious, especially in the transition region of long and short wave.

Note that the high refractive index of k9 glass will cause obvious reflection effects, so there is actually a polarization-insensitive anti-reflection coating on the back surface of the substrate.

Conclusion

The polarization deviation at oblique incidence is a common condition, which will cause the deterioration of optical system performance in most cases. Especially in the full polarization detection system, this deviation will affect the accuracy of information detection, so polarization-insensitive film filters are crucial.

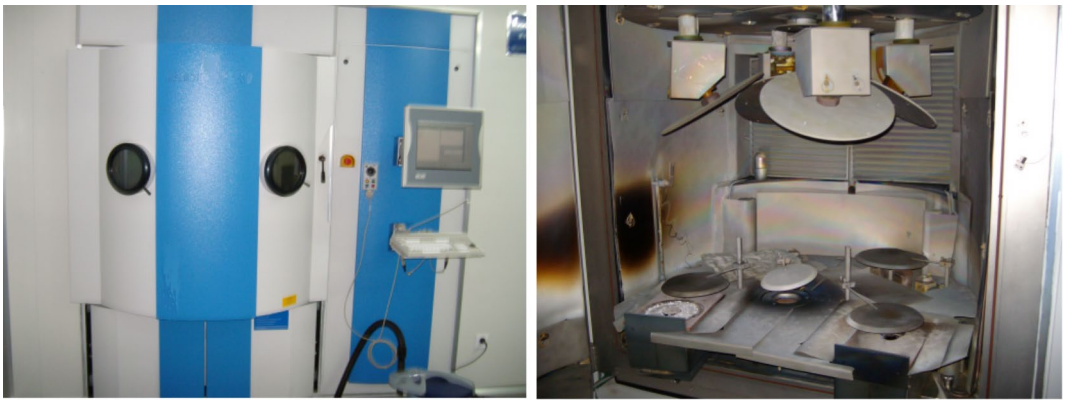

Fig. 8. SYRUSpro1110 high vacuum coating machine (**a**) front surface (**b**) vacuum chamber.

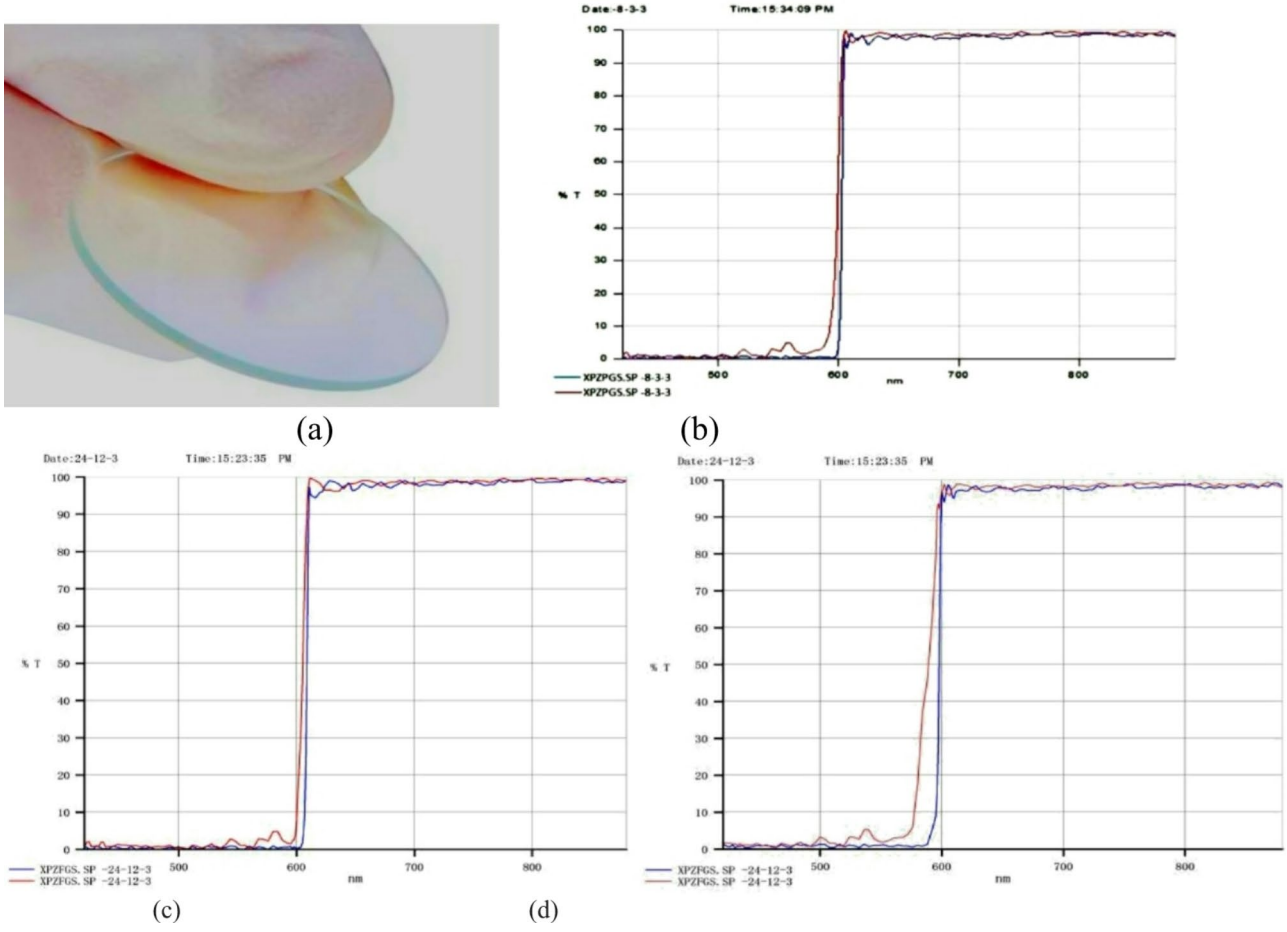

Fig. 9. Final physical photo and corresponding measured spectral transmittance of the splitter. (**a**) Physical photo (**b**, **c**, **d**) Transmittance curve of 45 degrees, 42 degrees, 48 degrees respectively.

In this paper, based on the symmetric structure with the matching layers, a polarization insensitive splitter with three all-dielectric material is designed and fabricated. In terms of theoretical performance statistics, the average reflectance of S-polarized and P-polarized light in the short-wave region of 420 to 580 nm is 97.8825% and 96.8038% respectively. And the average transmittance of S-polarized and P-polarized light in the long-wave region of 620 to 880 nm is 98.2491% and 99.2975% respectively. From the experimental transmittance curve, the overall agreement between measured curves and theoretical performance statistics is relatively good, although the reflectance and transmittance have a small decrease. It can to say, in the working range of spectrum, the

design maintains a very low polarization ratio, which will reduce the difficulty of interpreting the information with full polarization detection technology.

Through the work of this paper, we can conclude that the initial film stack suitable for polarization-insensitive cutoff filters can be obtained by combining the symmetric structure and matching layer composed of three materials. This provides a suitable initial value for the optimization algorithm, and it only needs to be slightly optimized by the traditional optimization algorithm to get the design suitable for the target. Moreover, the design does not have ultra-thin layers and can be successfully produced using existing coating technology. However, unfortunately, this design is not suitable for polarization-insensitive splitters with specific spectral ratio requirements, and we will further pursue related research.

Data availability

The data that support the findings of this study are available from the corresponding author upon reasonable request.

Received: 20 August 2024; Accepted: 12 February 2025
Published online: 18 February 2025

References

1. Jonušauskas, L. et al. Femtosecond laser-made 3D micro-chainmail scaffolds towards regenerative medicine. *Opt. Laser Technol.* **162**, 109240 (2023).
2. Shen, F. et al. Impact of lock-in time constant on remote monitoring of trace gas in the atmospheric column using laser heterodyne radiometer (LHR). *Remote Sens.* **14**(12), 2923 (2022).
3. Kaushal, H. & Kaddoum, G. Applications of lasers for tactical military operations. *IEEE Access* **5**, 20736–20753 (2017).
4. Hu, C. et al. High-resolution, multi-frequency and full-polarization radar database of small and group targets in clutter environment. *Sci. China Inf. Sci.* **66**, 227301 (2023).
5. Xing, S. et al. Full polarization states modulating via an ultra-thin quarter-wave plate. *Eur. Phys. J. D* **75**, 87 (2021).
6. Kang, M. et al. Coherent full polarization control based on bound states in the continuum. *Nat. Commun.* **13**, 4536 (2022).
7. Yao, D., Liang, H. & Campos, J. Calculation and restoration of lost spatial information in division-of-focal-plane polarization remote sensing using polarization super-resolution technology. *Int. J. Appl. Earth Observ. Geoinf.* **116**, 103155 (2023).
8. Yan, L. et al. General review of optical polarization remote sensing. *Int. J. Remote Sens.* **41**(13), 4853–4864 (2020).
9. El-Ocla, H. Accurate remote sensing of conducting objects in random media with plane H-wave polarization. *J. Electromagn. Waves Appl.* **33**(7), 799–810 (2019).
10. Ishizuka, N., Li, J., Fuji, W., Ikezawa, S. & Iwami, K. Linear polarization-separating metalens at long-wavelength infrared. *Optics Express* **31**(14), 23372–23381 (2023).
11. Rego, L., Smirnova, O. & Ayuso, D. Tilting light's polarization plane to spatially separate the ultrafast nonlinear response of chiral molecules. *Nanophotonics* **12**(14), 2873–2879 (2023).
12. Ba, D., Hua, Z., Li, Y. & Dong, Y. Polarization separation assisted optomechanical time-domain analysis with submeter resolution. *Optics Lett.* **46**(23), 5886–5889 (2021).
13. You, D. et al. Nb_2O_5 deposited by ion-assisted reactive magnetron sputtering for near-infrared optical coating: Power modulation and performance degradation. *Infrared Phys. Technol.* **135**, 104978 (2023).
14. Huang, Y.-S. et al. Tunable structural transmissive color in fano-resonant optical coatings employing phase-change materials. *Mater. Today Adv.* **18**, 100364 (2023).
15. Arne, R., Tore, K., Ørnulf, N. & Chang, C. Y. Optical interference coatings for coloured building integrated photovoltaic modules: Predicting and optimising visual properties and efficiency. *Energy Build.* **298**, 113517 (2023).
16. Hoa, P. V., Phi, N. T. & Gubanova, L. A. Nonpolarizing interference systems containing metallic layers. *Optics Spectroscopy* **127**(3), 581–585 (2019).
17. Willey, R. R. Building blocks for nonpolarizing optical coatings. *Appl. Optics* **47**(33), 6230–6235 (2008).
18. Thelen, A. Nonpolarizing interference films inside a glass cube. *Appl. Optics* **15**(12), 2983–2985 (1976).
19. Hecht, E. *Optics* 2nd edn. (Addison-Wesley, 1987).

Author contributions

Wang wenliang wrote the main manuscript text and prepared Figs. 1, 2, 3, 4, 5 and 6. All authors reviewed the manuscript.

Declarations

Competing interests

The authors declare no competing interests.

Additional information

Correspondence and requests for materials should be addressed to W.w.

Reprints and permissions information is available at www.nature.com/reprints.

Publisher's note Springer Nature remains neutral with regard to jurisdictional claims in published maps and institutional affiliations.